Asymptotic Stabilization of an Active Magnetic Bearing System using LMI-based Sliding Mode Control

Abdul Rashid Husain, Mohamad Noh Ahmad, and Abdul Halim Mohd. Yatim

Abstract—In this paper, stabilization of an Active Magnetic Bearing (AMB) system with varying rotor speed using Sliding Mode Control (SMC) technique is considered. The gyroscopic effect inherited in the system is proportional to rotor speed in which this nonlinearity effect causes high system instability as the rotor speed increases. Also, transformation of the AMB dynamic model into a new class of uncertain system shows that this gyroscopic effect lies in the mismatched part of the system matrix. Moreover, the current gain parameter is allowed to be varied in a known bound as an uncertainty in the input matrix. SMC design method is proposed in which the sufficient condition that guarantees the global exponential stability of the reduced-order system is represented in Linear Matrix Inequality (LMI). Then, a new chattering-free control law is established such that the system states are driven to reach the switching surface and stay on it thereafter. The performance of the controller applied to the AMB model is demonstrated through simulation works under various system conditions.

Keywords—Active Magnetic Bearing (AMB), Sliding Mode Control (SMC), Linear Matrix Inequality (LMI), mismatched uncertainty.

I. INTRODUCTION

SLIDING Mode Control (SMC) has received great attention in recent years because of its robustness against uncertainties present in system [1], [2] ,[3] and [4]. SMC is a nonlinear control technique that is applicable to a wide range of dynamic system including the linear, nonlinear, multi-input/multi-output, discrete-time and large scale systems. There are many approaches have been reported and considered in the design process of the sliding-mode control law, such that the system is robust or even insensitive to parametric uncertainties and disturbance. In the practical application of SMC, the controller has also been successfully adapted in many forms and applied in numerous real-world applications such as robot manipulator [5], active suspension system [6], magnetic suspension system and magnetic bearings [7][8].

The design of SMC controller involves two crucial steps which are commonly referred to as the reaching phase and the sliding phase [1][2]. In this paper, the design of both the sliding surface and control law based on SMC theory and its application to a five-degree-of-freedom (5 DOF) AMB system reported in [8] are considered. The AMB system contains the gyroscopic effect in which this nonlinearity causes the system to be unstable and the magnitude is proportional to the rotating speed of the rotor. Also, in this work, the linearized current-force factor of the AMB system is allowed to be varied by 20% of its nominal value. This relaxed condition is introduced to accommodate some variations in the range of the value of this parameter that is originally obtained through experimental set-up. After transforming the system into a regular form, a new class of dynamic system is formed in which it is shown that the gyroscopic effect belongs to mismatched uncertainty while the uncertain value of current-force factor is matched. Based on this new system model, a sufficient condition is established such that the reduced-order system with the present of these uncertainties, when restricted to the switching surface, is guaranteed to achieve global stability. This sliding condition is formulated in term of Linear Matrix Inequality (LMI) in which various powerful semi-definite programming methods are available to find the desired optimal solution, which consequently yields fully parameterized sliding surface. Subsequently, a new control law is designed such that the system states are driven to the sliding surface and to remain on it thereafter. In order to make the controller to be more practical, the boundary layer technique is also adapted in the nonlinear switching term in which the input chattering is eliminated while the robustness of the system is still maintained.

The outline of this paper is as follows: In Section II, the model of the AMB system based on [8] is illustrated and represented in its deterministic form which serves as a tool for the controller design. Section III covers the detail design of SMC control algorithm wherein both the parameterization of sliding surface in term of LMIs and the development of nonlinear control law are shown. The stability of the system under the designed controller is also shown. Then, in Section IV, the performances on the AMB system under the designed controller are illustrated through simulation works under various system conditions. Finally, the conclusion in Section V summarizes the contribution of the work.

A. R. Husain is with Universiti Teknologi Malaysia (UTM), 81310, Skudai, Johore Malaysia (phone: +607-5535894; fax: +607-5566272; e-mail: rashid@ fke.utm.my).

M. N. Ahmad is with Universiti Teknologi Malaysia (UTM), 81310, Skudai, Johore Malaysia. He is the Head of Dept. Mechatronics and Robotics, Faculty of Elec. Eng., UTM (e-mail: noh@fke.utm.my).

A. H. M. Yatim is with the Universiti Teknologi Malaysia (UTM), 81310, Skudai, Johore Malaysia.. He is the Deputy Dean (Academics), Faculty of Elec. Eng., UTM (e-mail: halim@ieee.org).

II. MODELING OF AN ACTIVE MAGNETIC BEARING SYSTEM

In order to synthesize the proposed sliding surface with the controller, a vertical shaft AMB system model for the application of turbo molecular pump system is re-derived based on the work done in [8].
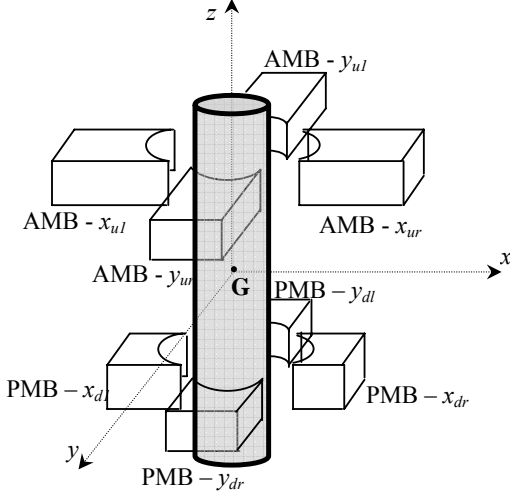
A. Mathematical Model

Fig. 1 Vertical Active Magnetic Bearing System

The gyroscopic effect that causes the coupling between two axes of motions (pitch and yaw). Fig. 1 illustrates the five DOF vertical magnetic bearing in which the vertical axis (z-axis) is assumed to be decoupled from the system and hence
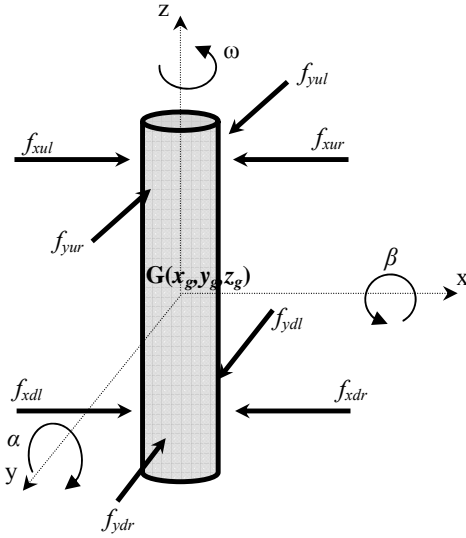

Fig. 2 AMB free-body diagram

controlled separately. The top part of the rotor of the system in Fig. 1 is controlled actively by the magnetic bearing, labeled as AMB, in which the coil currents are the inputs. The bottom part of the rotor however is levitated to the center of the system by using two sets of permanent magnets labeled as

PMB. The rotation of rotor around the z-axis is supplied by external driving mechanism and considered as a time-varying parameter.

Fig. 2 illustrates the free-body diagram of the rotor which shows the total forces produced by the AMB and PMB of the system. Based on the principle of flight dynamics [9], the equations of motion of the rotor-magnetic bearing system is as follows:

$$
\begin{aligned}
m\ddot{x}_g &= f_{x_u} + f_{x_b} \\
J_r\ddot{\beta} &= -J_a\omega_z\dot{\alpha} + L_u f_{x_u} - L_b f_{x_b} \\
m\ddot{y}_g &= f_{y_u} + f_{y_b} \\
J_r\ddot{\alpha} &= J_a\omega_z\dot{\beta} - L_u f_{y_u} + L_b f_{y_b}
\end{aligned}
\tag{1}
$$

The gyroscopic effect is represented by the term $-J_a\omega_z\dot{\alpha}$ and $J_a\omega_z\dot{\beta}$, where it can be noticed that this will cause the coupling between the axes of motions proportional to the speed. The control forces produced by the AMB are given by the following equations:

$$
\begin{aligned}
f_{xu} &= 2K_{du}x_g + 2L_u K_{du}\beta + 2K_{iu}I_x \\
f_{yu} &= 2K_{du}y_g - 2L_u K_{du}\alpha + 2K_{iu}I_y
\end{aligned}
\tag{2}
$$

where $f_{xu} = f_{xur} - f_{xul}$ and $f_{yu} = f_{yur} - f_{yul}$ are the net forces produced by the AMB on each x- and y-axis respectively (the same net force for bottom PMB as well). This is possible by having the AMB coil wound to produce differential current mode. For the PMB, the net forces produced are given by the following equations:

$$
\begin{aligned}
f_{xb} &= -2C_b\dot{x}_g + 2C_b L_b\dot{\beta} - 2K_b x_g + 2K_b L_b\beta \\
f_{yb} &= -2C_b\dot{y}_g - 2C_b L_b\dot{\alpha} - 2K_b y_g - 2K_b L_b\alpha
\end{aligned}
\tag{3}
$$

Equations (1), (2) and (3) can be integrated to produce the AMB model in the following form:

$$
\dot{X}(t) = A(\omega)X(t) + BU(t)
\tag{4}
$$

where $X = [x_g, \beta, y_g, \alpha, \dot{x}_g, \dot{\beta}, \dot{y}_g, \dot{\alpha}]^T$ are the states of the system, $A(\omega) \in \Re^{8x8}$ is the system matrix, $B \in \Re^{8x2}$ is the input matrix, $U(t) = [I_x \ I_y]^T$ the input currents. The nonzero elements of the matrices are shown in the appendix. In, this study, the current-to-force parameter, K_{ix}, is allowed to vary about 20% from its nominal value. This condition is introduced since the parameter value is obtained from a linearized relation wherein some inaccuracies might occur. With this newly introduced condition, the controller designed in the following section is formulated to be robust towards not only the gyroscopic effect, but also this parametric uncertainty. Since the parameter, K_{ix}, is in the input matrix, the new AMB model can be represented as follows:

$$
\dot{X}(t) = [A + \Delta A(\omega)]X(t) + [B + \Delta B(K_{ix})]U(t)
\tag{5}
$$

where $\Delta A(\omega)$ and $\Delta B(K_{ix})$ represent the uncertainties due to gyroscopic effect and parameter variation, respectively.

B. AMB Mode in Deterministic Form

In order to synthesize the controller, the AMB model is treated as an uncertain system in which deterministic approach to classify the system is used based on [10]. The model shown in (5) is readily in the uncertain class of system in which matrices A and B are the nominal constant matrices of the system. The decomposition into this deterministic form is possible due to the fact that the maximum and minimum values of the rotational rotor speed and the bound of the parameter variation are known. For this AMB model specifically, the elements of the $\Delta A(\omega,t)$ can be calculated based on these available bounds. The rotational speed is given as follows:

$$0 \; rpm \le \omega \le 20,000 \; rpm \; . \tag{6}$$

Symbol	Parameter	Value	Unit
m	Mass of Rotor	1.595	kg
J_a	Moment of Inertia about rotational axis	1.61×10^{-3}	kg.m^2
J_r	Moment of Inertia about radial axis	3.83×10^{-3}	kg.m^2
L_u	Distance of upper AMB to G	0.0128	m
L_b	Distance of lower PMB to G	0.0843	m
K_{iu}	Linearized force/current factor	200	N/A
K_{du}	Linearized force/displ. factor	2.8×10^5	N/m
K_b	Stiffness coefficient of PMB	1.0×10^5	N/m
C_b	Damping coefficient of PMB	48	kg/s
m_{un}	Static imbalance	0.6×10^{-3}	m
l	Distance of unbalance mass from G	0.02	m
ω	Rotor rotational speed	0 – 1047 (0 – 10000)	rad/sec (rpm)

Then, by using these bounds and the other system parameter values as shown in Table I, each element of the system matrix can be calculated and specified in the following form:

$$\underline{a}_{ij} \le a_{ij} (\omega,t) \le \overline{a}_{ij} \tag{7}$$

for $i = 1, \ldots, 8$, and $j = 1, \ldots, 8$, where $a_{ij}(\omega,t)$ are the element of $\Delta A(\omega,t)$ matrix. The upper and lower bars indicate the maximum and minimum values of the elements. The element of matrix A and $\Delta A(\omega,t)$ can be calculated based on these bounds by using the following equation:

$$a_A(i,j) = \frac{\overline{a}_{ij} + \underline{a}_{ij}}{2} \; , \; a_{\Delta A}(i,j) = \overline{a}_{ij} - a_A(i,j) \tag{8}$$

for i-th row,j-th column elements of A and $\Delta A(\omega,t)$.

For the uncertainty due to the parametric variation, $\Delta B(K_{ix})$, as it is assumed in this work that the value is varied by 20% of its nominal value and this value represents the highest bound of the uncertainty. Thus this is adequate for the controller design.

III. SLIDING MODE CONTROL DESIGN

Consider a class of uncertain systm

$$\dot{x}(t) = (A + \Delta A(x,p,t))x(t) + (B + \Delta B(x,p,t))u(t) \tag{9}$$

where $x(t) \in \mathfrak{R}^n$ is the system states, $u(t) \in \mathfrak{R}^m$ is the control input and p is any time-varying scalar function. A and B is the system and input matrices, respectively, and B is of full rank. $\Delta A(x,p,t)$ and $\Delta B(x,p,t)$ represent the uncertainties in the system matrix and input matrices. To complete the description of the uncertain dynamical system, the following assumptions are introduced and assumed to be valid.

A1) For existence purposes, $\Delta A (\cdot,\cdot,\cdot)$ and $\Delta B (\cdot,\cdot,\cdot)$ are continuous on their arguments.

A2) There exist known positive scalars γ_1 and γ_2 and a function $h(x,p,t)$ such that

$$\|\Delta A(x,p,t)\| \le \gamma_1 ,$$
$$\Delta B(x,p,t) = Bh(x,p,t) ,$$
$$\|h(x,p,t)\| \le \gamma_2 < 1 .$$

A3) The pair (A,B) is controllable.

Define a linear switching surface as

$$\sigma = Sx = 0 \tag{10}$$

where $S \in \mathfrak{R}^{m \times n}$ is of full row rank m. By referring to previous results [1][2][4], the switching surface parameter matrix S should be selected such that

E1) The matrix SB is nonsingular

E2) The reduced $(n-m)$ order system of the system (9) restricted on the switching surface $Sx=0$ is globally exponentially stable for all allowable uncertainties satisfying assumption A2).

A. The Design of the Sliding Surface

Let $\Phi \in \Re^{n \times (n-m)}$ be any full column rank matrix such that $B^T \Phi = 0$ and $\Phi^T \Phi = I_{n-m}$. Then it can be established that

$$\begin{bmatrix} \Phi^T \\ (B^T B)^{-1} B^T \end{bmatrix} \begin{bmatrix} \Phi & B \end{bmatrix} = \begin{bmatrix} I_{n-m} & 0 \\ 0 & I_m \end{bmatrix} \quad (11a)$$

or equivalently

$$\Phi^T \Phi + B(B^T B)^{-1} B^T = I_n. \quad (11b)$$

From this, it is obvious that the nonsingular transformation matrix can be defined as follows:

$$T = \begin{bmatrix} \Phi^T \\ (B^T B)^{-1} B^T \end{bmatrix} \quad (12)$$

Substituting (12) into system (9) gives

$$\dot{x}(t) = (A + \Phi \Phi^T \Delta A(x,p,t))x(t) + B\{[I + h(x,p,t)]u(t) \\ + (B^T B)^{-1} B^T (\Delta A(x,p,t)x\} \quad (13)$$

This new system representation has mapped the uncertainties into the matched and mismatched components in which it is obvious that $\Delta A(x,p,t)$ and $\Delta B(x,p,t)$ belong to the mismatched and matched components, respectively. This, however, will be more obvious as the stability analysis of the system on the switching surface is performed next.

Theorem 1. *Consider the system (9) and suppose assumption (A1)-(A3) hold. Then there exist a matrix S satisfying (E1) and (E2), if there is a matrix P > 0 and positive scalar δ such that*

$$\Phi^T A^T \Phi P + P \Phi^T A \Phi + \delta^{-1} P^2 \\ - (\delta \gamma_1)^{-1} P \Phi^T AB (B^T B)^{-1} B^T A^T \Phi P + (\delta \gamma_1^2) I_{n-m} < 0 \quad (14)$$

where γ_1 is given in assumption (A2). Moreover, the matrix S can be proposed to be as follows:

$$S = (B^T B)^{-1} B^T (I_n + (\delta \gamma_1^2)^{-1} A^T \Phi P \Phi^T) \quad (15)$$

Proof From (15) and $B^T \Phi = 0$, it is obvious that $SB = I_m$ and therefore condition (E1) is satisfied. And from $\Phi^T \Phi = I_{n-m}$, it is also true that

$$S\Phi = (\delta \gamma_1^2 B^T B)^{-1} B^T A^T \Phi P \quad (16)$$

By using the nonsingular transformation (12) in which a new state variable can be introduced such that $z = Tx = [x^T \Phi, x^T B (B^T B)^{-1}]^T = [z_1^T, z_2^T]^T$, system (9) can be transformed into the following regular form:

$$\dot{z}_1 = \Phi^T A \Phi z_1 + \Phi^T AB z_2 + \Phi^T \Delta A(x,p,t)x$$
$$\dot{z}_2 = (B^T B)^{-1} B^T A \Phi z_1 + (B^T B)^{-1} B^T AB z_2 \\ + (B^T B)^{-1} B^T \Delta A(x,p,t)x + (I_m + h(x,p,t))u \quad (17)$$

When the system (17) is restricted on the switching surface (10), then from $z = Tx$ it is known that $SM^{-1}z = 0$, i.e. $S\Phi z_1 + SB z_2 = 0$. With $SB = I_m$, it is obtained that $z_2 = -S\Phi z_1$. Then the reduced-order system (17) on the surface (10) is

$$\dot{z}_1 = (\Phi^T A \Phi - \Phi^T AB S\Phi)z_1 + \Phi^T \Delta A(x,p,t)x \quad (18)$$

where it is apparently clear that the uncertainty $\Delta A(x,p,t)$ present in (18) affects the stability of the system. Then, take $V(z_1) = z_1^T P z_1$ as a Lyapunov candidate function, then the derivative of $V(z_1)$ along (18) is derived to be

$$\dot{V}(z_1) = z_1^T [\Phi^T A \Phi - \Phi^T AB S\Phi]^T P + P(\Phi^T A \Phi - \Phi^T AB S\Phi)]z_1 \\ + 2z_1^T P \Phi^T \Delta A(x,p,t)x \quad (19)$$

From $x = M^{-1}z = \Phi z_1 + B z_2$ and $z_2 = -S\Phi z_1$, it can be shown that $x = (\Phi - SB\Phi)z_1$. Together with $B^T \Phi = 0$ and $\Phi^T \Phi = I_{n-m}$, the last term of (19) can be reduced as follows:

$$2z_1^T P \Phi^T \Delta A(x,p,t)x$$
$$\leq \frac{1}{\delta} z_1^T P \Phi^T \Phi P z_1 + \delta x^T \Delta A(x,p,t)^T \Delta A(x,p,t)x$$
$$\leq \frac{1}{\delta} z_1^T P^2 z_1 + \delta \|\Delta A(x,p,t)\|^2 \|x\|^2$$
$$\leq \frac{1}{\delta} z_1^T P^2 z_1 + \delta \gamma_1 x^T x$$
$$= \delta^{-1} z_1^T P^2 z_1 + \delta \gamma_1 z_1^T (\Phi - SB\Phi)^T (\Phi - SB\Phi)z_1$$
$$= z_1^T (\delta^{-1} P^2 + \delta \gamma_1^2 I_{n-m} + \delta \gamma_1^2 \Phi^T S^T B^T BS\Phi)z_1$$

where δ is any positive scalar. Thus, the derivative of the Lyapunov candidate function (19) is

$$\dot{V}(z_1) \leq z_1^T \Sigma z_1 \quad (20)$$

where

$$\Sigma = (\Phi^T A \Phi - \Phi^T AB S\Phi)^T P + P(\Phi^T A \Phi - \Phi^T AB S\Phi) \\ + (\delta^{-1} P^2 + \delta \gamma_1^2 I_{n-m} + \delta \gamma_1^2 \Phi^T S^T B^T BS\Phi) \\ = \Phi^T A^T \Phi P + P \Phi^T A \Phi + \delta^{-1} P^2 + \delta \gamma_1^2 I_{n-m} - \Phi^T S^T B^T A^T \Phi P \\ + \delta \gamma_1^2 \Phi^T S^T B^T BS\Phi - P \Phi^T AB S\Phi \\ = \Phi^T A^T \Phi P + P \Phi^T A \Phi + \delta^{-1} P^2 + \delta \gamma_1^2 I_{n-m} \\ - (\delta \gamma_1^2)^{-1} P \Phi^T AB (B^T B)^{-1} B^T A^T \Phi P + \{\Phi^T S^T \\ - P \Phi^T AB (\delta \gamma_1^2 B^T B)^{-1}\}[\delta \gamma_1^2 (B^T B)]\{S\Phi \\ - (\varepsilon \gamma_1^2 B^T B)^{-1} B^T A^T \Phi P\}$$

By using (16), this is further reduced to

$$\Sigma = \Phi^T A^T \Phi P + P\Phi^T A\Phi + \delta^{-1}P^2 + \delta\gamma_1^2 I_{n-m}$$
$$- (\delta\gamma_1^2)^{-1}P\Phi^T AB(B^T B)^{-1}B^T A^T \Phi P.$$

Thus, (20) together with (14) and $P > 0$ implies that the reduced-order system (18) achieves global exponential stability when sliding on the surface (10). This completes the proof of Theorem 1. □

Finding the solution of the Riccati inequality (14) usually gives a non-unique solution such that the conditions set are met. This however can be improved in which the solution not only fulfill (14) but also the trace of the solution is minimized. This is proven to be advantageous particularly for AMB system since the control effort is also reduced. This problem can be reformulated in term of LMI and stated in the following lemma.

Lemma 1. *The existence solution (14) is equivalent to solving the following LMI set which is:*

$$\begin{bmatrix} \overline{A}^T P + P\overline{A} + \overline{C} & P\Phi^T \\ \Phi P & V^{-1} \end{bmatrix} < 0 \qquad (21)$$

$$P > 0 \qquad (22)$$

where

$$\overline{A} = \Phi^T A\Phi,$$
$$\overline{C} = \delta\gamma_1^2 I_{n-m},$$
$$V = \delta\gamma_1^2 AB(B^T B)^{-1}B^T A^T - \delta^{-1}.$$

Proof   From (14) and $\Phi^T \Phi = I_{n-m}$, the following inequality is produced

$$\Phi^T A^T \Phi P + P\Phi^T A\Phi + (\delta\gamma_1^2)I_{n-m}$$
$$- P[(\delta\gamma_1)^{-1}\Phi^T AB(B^T B)^{-1}B^T A^T \Phi - \delta^{-1}\Phi^T \Phi]P < 0$$
$$[\Phi^T A\Phi]^T P + P[\Phi^T A\Phi] + (\delta\gamma_1^2)I_{n-m}$$
$$- P\Phi^T[(\delta\gamma_1)^{-1}AB(B^T B)^{-1}B^T A^T - \delta^{-1}]\Phi P < 0.$$

By using Schur complement [11][12], the above LMI set is obtained and this complete the proof. □

B. Synthesis of Control Law

To find the control law such the trajectories of system (9) are driven to the designed sliding surface and to remain on the surface for the subsequent time, the following reachability condition is used [2][4]

$$\sigma^T \dot{\sigma} \leq -\beta\|\sigma\| \qquad (23)$$

where β is a positive scalar and σ is the sliding surface defined by (10). With this reaching condition the following theorem can be introduced.

Theorem 2. *Consider system (9) with the assumption A1) and A2). If the LMI set (21) and (22) has a solution and the sliding surface S is solvable given by (15), the reachability condition (23) is satisfied by employing the control law given below:*

$$u(t) = -SAx - \frac{1}{(1-\gamma_2)}\{[\gamma_1\|S\| + \gamma_2\|SA\|]\|x\| + \beta\}\frac{\sigma}{\|\sigma\|} \qquad (24)$$

where S is given by (15) and β is a designed positive scalar.

Proof   To proof this theorem, the reachability condition (23) for system (9) with control law (24) and $SB = I_m$ is used. From (23), it can be shown that

$$\sigma^T \dot{\sigma} = \sigma^T S([A + \Delta A(x,p,t)]x + B[I_m + h(x,p,t)]u)$$
$$= \sigma^T (SAx + S\Delta A(x,p,t)x + u + h(x,p,t)u)$$
$$= \sigma^T (SAx + S\Delta A(x,p,t)x + h(x,p,t)u$$
$$- SAx - \frac{1}{(1-\gamma_2)}\{[\gamma_1\|S\| + \gamma_2\|SA\|]\|x\| + \beta\}\frac{\sigma}{\|\sigma\|})$$
$$= \sigma^T (S\Delta A(x,p,t)x + h(x,p,t)u) - \frac{1}{(1-\gamma_2)}[\gamma_1\|S\|$$
$$+ \gamma_2\|SA\|]\|x\|\|\sigma\| - \frac{1}{(1-\gamma_2)}\beta\|\sigma\|$$
$$\leq \|S\|\|\Delta A(x,p,t)\|\|x\|\|\sigma\| + \|h(x,p,t)\|\|u\|\|\sigma\| - \frac{1}{(1-\gamma_2)}[\gamma_1\|S\|$$
$$+ \gamma_2\|SA\|]\|x\|\|\sigma\| - \frac{1}{(1-\gamma_2)}\beta\|\sigma\|$$

From (24), it is known that

$$\|u\| \leq \|SA\|\|x\| + \frac{1}{(1-\gamma_2)}[\gamma_1\|S\| + \gamma_2\|SA\|]\|x\| + \frac{1}{(1-\gamma_2)}\beta.$$

With this inequality, the reachability condition can further be simplified to be

$$\sigma^T \sigma \leq -\frac{\gamma_1\gamma_2}{(1-\gamma_2)}\|S\|\|x\|\|\sigma\| + \gamma_2\|SA\|\|x\|\|\sigma\| + \frac{\gamma_2}{(1-\gamma_2)}\beta\|\sigma\|$$
$$+ \frac{\gamma_2}{(1-\gamma_2)}(\gamma_1\|S\| + \gamma_2\|SA\|)\|x\|\|\sigma\| - \frac{\gamma_2}{(1-\gamma_2)}\|SA\|\|x\|\|\sigma\|$$
$$- \frac{1}{(1-\gamma_2)}\beta\|\sigma\|$$
$$\leq (\gamma_2 + \frac{\gamma_2^2}{(1-\gamma_2)} - \frac{\gamma_2}{(1-\gamma_2)})\|SA\|\|x\|\|\sigma\| + \frac{(\gamma_2-1)}{(1-\gamma_2)}\beta\|\sigma\|$$
$$\leq -\beta\|\sigma\|$$

Thus, the reachability condition (23) is satisfied and the proof of Theorem 2 is complete. □

It is well known that the discontinuous control term in (24) introduces high chattering effect which is undesirable in any dynamic system due to its infinite switching frequency. This high frequency switching input can excite any high-frequency

unmodelled dynamics in the system and cause system instability [1][2]. To overcome this chattering effect, the boundary layer technique is used instead of the discontinuous term as covered in [13]. The new control law adapting the boundary layer techniques is as below:

$$u(t) = -SAx - \frac{1}{(1-\gamma_2)}\{[\gamma_1\|S\| + \gamma_2\|SA\|]\|x\| + \beta\}sat(\frac{\sigma}{\Pi}) \quad (25)$$

where Π is the thickness of the boundary layer. The detail of the selection of the Π value and its relation towards the trade-off of the robustness of the system is discussed in detail in [13] and intentionally omitted in this work. The adaptation of the method is purely to produce a control law that is chattering-free which is more practical for actual application.

IV. SIMULATION ON AMB SYSTEM AND DISCUSSION

The simulation work is performed by using MATLAB® and Simulink®. For solving the LMI problem (21) and (22), instead of using standard LMI Toolbox in Matlab, YALMIP/SeDuMi convex problem solver for semi-definite problem is used [14][15]. YALMIP/SeDuMi is among the newly developed convex problem solver which is proven to produce a less conservative solution and a higher convergence rate. This makes it very attractive especially for designing the controller which in nature a reduced conservatism is practically preferable. After transformation of the AMB model into the deterministic form, the procedure of designing the controller and its application on the system is outlined as follows:

Step 1: Compute the norm for the system matrix uncertainty $\Delta A(\omega,t)$:

$$\|\Delta A\| = 440.1223 \quad \|h(x,p,t)\| \le 0.2$$

Note that the variation of parameter K_{ix} is already assumed to be 20% varying from its nominal value. Thus, it is explicitly known that the norm for the function, $h(x,p,t)$, which bound the uncertainty in the B matrix is 0.2. With these norm bounded values, the constant in assumption $A2$) are as follows:

$$\gamma_1 = 440.1223, \gamma_2 = 0.2.$$

Step 2: Solve LMI sets (21) and (22) for P (with $\delta = 1$) to parameterize the sliding surface, S in (15).

By using the YALMIP/SeDuMi LMI solver, the value for the matrix P is as follows:

$$P = \begin{bmatrix} 1.1587\times10^4 & * & * & * & * & * \\ 6.970\times10^4 & 5.9141\times10^4 & * & * & * & * \\ 1.5003\times10^4 & 1.1864\times10^4 & 1.1203\times10^4 & * & * & * \\ 2.8668\times10^4 & 2.2114\times10^4 & 5.8769\times10^4 & 2.8014\times10^4 & * & * \\ 0 & 0 & 0 & 0 & 0 & * \\ 0 & 0 & 0 & 0 & 0 & 0 \end{bmatrix}$$

where (*) indicates the symmetrical values. With this P, the surface parameter is calculated to be as follows:

$$S = 10^{-4}\begin{bmatrix} 3 & 23 & 5 & 8 & 1 & 7 & 0 & -3 \\ -1 & -7 & -1 & 10 & 0 & 0 & 15 & 1 \end{bmatrix}$$

Step 3: Select parameter β and Π for controller (25).

Parameter $\beta = 0.2$ is chosen. Any small positive value such that reachability is met is adequate for the design. For the boundary layer, Π, it does affect the performance of the control in which the bigger the value is, the less chattering will occur in the control current I_x. However, the trade-off is, less robustness is noticed since instead of reaching the stable sliding surface, the states trajectories enter and oscillate in the given boundary [13]. For this work two Π values are chosen which are $\Pi = 10^5$ and $\Pi = 10^3$ to illustrate the effect on the system.

The initial values of the states are set at $[x_g, \beta, y_g, \alpha, \dot{x}_g, \dot{\beta}, \dot{y}_g, \dot{\alpha}]^T$ = $[2\times10^{-4}$ m,-2×10^{-5} rad,1×10^{-4} m,$0,0,0,0,0]^T$. Fig. 3 shows the trajectories of states X and Y settle to zero when the rotor speed, $\omega = 10,000$rpm is set, the nominal value rotor speed. Also, the current-to-force parameter, K_{ix}, is set to its nominal value with no variation of its value. All other states also converge to zero but only X and Y values are shown due to their relatively large initial values.

In Fig. 4, the variation of 20% of K_{ix} value is introduced into the AMB model and it is proven that the system is robust under the new control law as the trajectories of X and Y in which the difference is hardly noticeable compared to Fig. 3. As the rotor speed is increased to its maximum value, 20,000rpm, the magnitude of the oscillations of X and Y at the beginning stage is insignificantly higher as shown in Fig. 5. With the results shown in these three figures, it is proven that under the control law (25), the system is robustly stable in a wide range of rotor speed as well as variation occurs in the K_{ix} value.
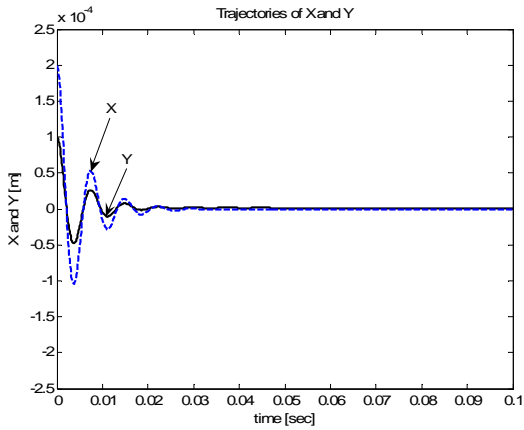
Fig. 3 X and Y trajectories with $\omega = 10$krpm, $\gamma_2 = 0$
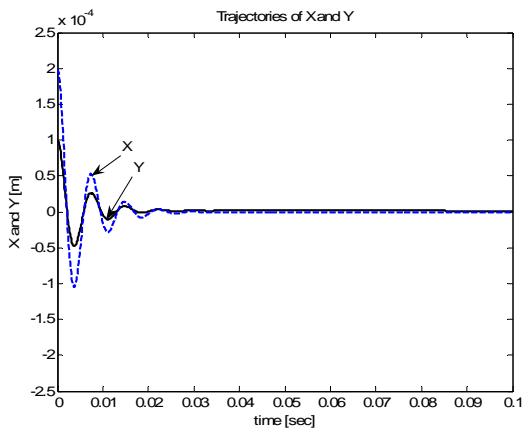
Fig. 4 X and Y trajectories with $\omega = 10$krpm, $\gamma_2 = 0.2$
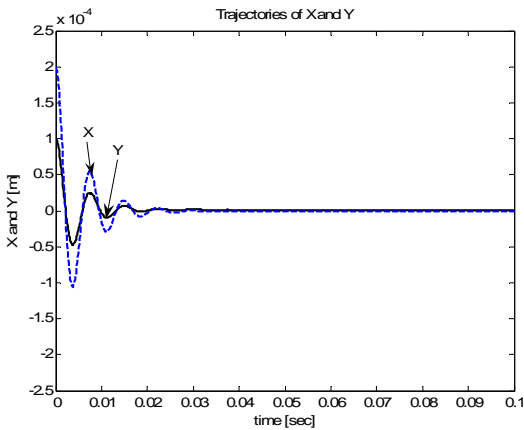
Fig. 5 X and Y trajectories with $\omega = 20$krpm, $\gamma_2 = 0.2$

When the boundary value Π is reduced from 10^5 to 10^3, the system will be more sensitive toward the uncertainties and this result is shown in Fig. 6 in which X and Y oscillate at higher amplitudes and take a longer time to settle to zero. The control current, Ix, for both of these boundary values are shown in Fig. 7 where it can be noticed the control effort for $\Pi = 10^3$ is higher in order to bring the states to zero. Finally, when the ideal switching control term (24) is used, a very high chattering effect can be seen as shown in Fig. 8. Although this control law provides the highest robustness of the system, as discussed earlier, it is very 'expensive' in term of practicality.
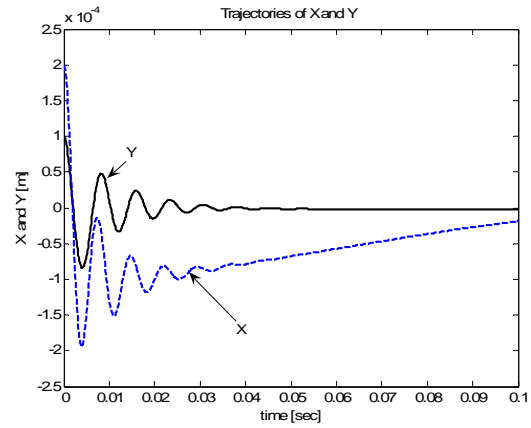
Fig. 6 X and Y trajectories with $\omega = 20$krpm, $\gamma_2 = 0.2$ and boundary layer $\Pi = 1000$
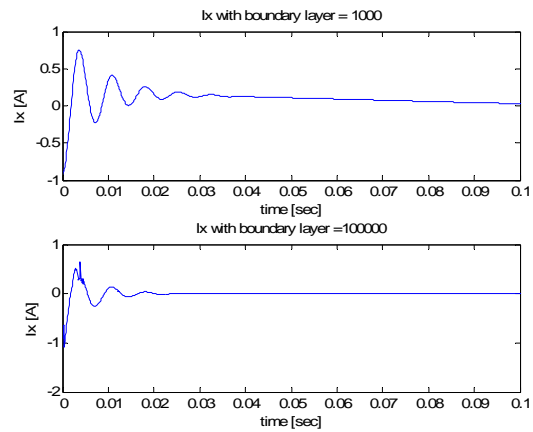
Fig. 7 Current I_x with $\Pi = 1000$ (top) and $\Pi = 100000$ (bottom)
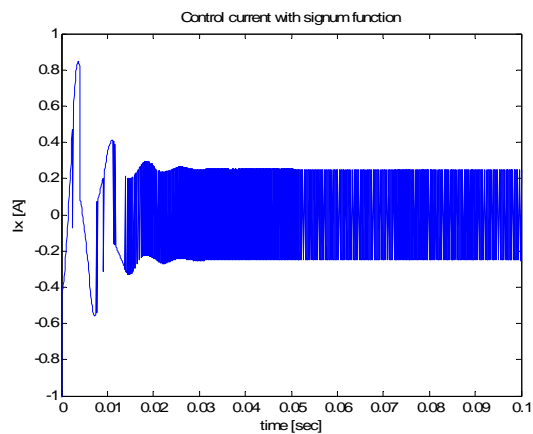
Fig. 8 Current I_x with discontinous term (signum function)

Remark Note that the norm of the control input is known to be as follows:

$$\|u\| \leq \|SA\|\|x\| + \frac{1}{(1-\gamma_2)}[\gamma_1\|S\| + \gamma_2\|SA\|]\|x\| + \frac{1}{(1-\gamma_2)}\beta.$$

and the term $\|SA\|$ and $\frac{1}{(1-\gamma_2)}[\gamma_1\|S\| + \gamma_2\|SA\|]$ which contain the surface parameter S, contribute significantly to the upper bound of the control effort. The Table II shows the values of these terms obtained from solving LMIs and algebraic Riccati equation (ARE) in which it shows that parameterization with the LMI solution produce a desirably lower control effort.

TABLE II
COMPARISON BETWEEN LMI AND ARE

Control term	LMI	ARE
$\|SA\|$	4.5708×10^3	4.5917×10^3
$\frac{1}{(1-\gamma_2)}[\gamma_1\|S\| + \gamma_2\|SA\|]$	1.1442×10^3	1.1494×10^3

V. CONCLUSION

In this work, a new chattering-free SMC controller is proposed for stabilization of a five-DOF AMB system in which sliding surface is designed based solving a set of LMIs. The proposed controller is proven to be able to achieve asymptotic stability at a wide range of rotational rotor speed although with the present of mismatched and matched system uncertainty. The performance of the controller is demonstrated through various simulation works.

APPENDIX

The nonzero elements of matrix $A(\omega,t)$, B where i and j indicate the i-th and j-th entry of each element.

$$a_{51} = \frac{2(K_{du} - K_b)}{m}, a_{52} = \frac{2(L_uK_{du} - L_bK_b)}{m}, a_{55} = \frac{2C_b}{m}, a_{56} = \frac{2C_bL_b}{m},$$

$$a_{61} = \frac{2(L_uK_{du} - L_bK_b)}{J_r}, a_{62} = \frac{2(L_u^2K_{du} - L_b^2K_b)}{J_r}, a_{65} = \frac{2L_bC_b}{J_r},$$

$$a_{66} = \frac{2L_b^2C_b}{J_r}, a_{68} = \frac{J_a}{J_r}p, a_{73} = \frac{2(K_{du} - K_b)}{m}, a_{74} = \frac{2(L_uK_{du} + L_bK_b)}{m},$$

$$a_{77} = \frac{2C_b}{m}, a_{78} = \frac{2C_bL_b}{m}, a_{83} = \frac{2(L_uK_{du} + L_bK_b)}{J_r}, a_{84} = \frac{2(L_u^2K_{du} - L_b^2K_b)}{J_r},$$

$$a_{86} = \frac{J_a}{J_r}p, \ a_{87} = \frac{2L_bC_b}{J_r}, a_{68} = \frac{2L_b^2C_b}{J_r}, b_{51} = b_{72} = \frac{2K_{iu}}{m}, b_{61} = -b_{82} = \frac{2L_uK_{iu}}{J_r}.$$

ACKNOWLEDGMENT

REFERENCES

[1] J. Y. Hung, W. B. Gao, and J. C. Hung, "Variable Structure control: A Survey," *IEEE Trans. Industrial. Electronics*, vol. 40, no. 1, pp. 2-22., 1993.

[2] S. Spurgeon, and C. Edwards, *Sliding Mode Control: Theory and Applications*. London: Taylor and Francis, 1998.

[3] X. Li, and R. A. DeCarlo, "Robust Sliding Mode Control of Uncertain Time Delay Systems," *Int. J. Control*, vol. 76, no. 13, pp. 1296-1305, 2003.

[4] X. Z. Dong, "State Feedback Sliding Mode Control for A Class of Systems with Mismatched Uncertainties and Disturbance," in *Proc. 25th Chinese Control Conference*, Heilongjiang, 2006, pp. 938-942.

[5] M. N. Ahmad, J. H. S. Osman, and M. R. A. Ghani, "Proportional-Integral Sliding Mode Tracking Controller with Application to a Robot Manipulator," in *7th Conf. on Contr., Auto., Rob and Sys., ICARCV*, Singapore, 2003, pp. 863-868.

[6] Y. M. Sam, and J. H. S. Osman, "Modeling and Control of Active Suspension System Using Proportional Integral Sliding Mode Approach," *Asian Jour. Contr.*, vol. 7, no. 2, pp. 91-98, 2005.

[7] J. H. Lee, P.E. Allaire, G. Tao, J. A. Decker, and X. Zhang, "Experimental Study of Sliding Mode Control for a Benchmark Magnetic Bearing System and Artificial Heart Pump Suspension," *IEEE Trans. on Contr. Sys. Mag*, vol. 11, no. 1, pp. 128-138, 2003.

[8] S. Sivrioglu, and K. Nonami, "Sliding Mode Control With Time-Varying Hyperplane for AMB Systems," *IEEE/ASME Trans. on Mechatronics*, vol. 3, no. 1, pp. 51-59, 1998.

[9] F. Matsumura, and T. Yoshimoto, "System modeling and control design of a horizontal shaft magnetic bearing system," *IEEE Trans. Magnetics*, vol. MAG-22, no. 3, pp. 196-203, May 1986.

[10] J. H. S. Osman, and P.D. Roberts, "Two Level Control Strategy for Robot Manipulators," *Int. Jour. of Control*, vol. 61, no. 6, pp. 1201 – 1222, 1995.

[11] S. Boyd, L. El Ghaoui, E. Feron, and V. Balakrishnan, *Linear Matrix Inequality in Systems and Control Theory*, Philadelphia: SIAM, vol. 15, 1994.

[12] J. G. VanAntwerp, and R. D. Braatz, "A Tutorial on Linear and Bilinear Matrix. *Int. Journal of Process Control*, vol. 10, pp. 363 – 385, 2000.

[13] D. Q. Zhang, and S. K. Panda, "Chattering-free and fast-response sliding mode controller," *IEEProc. –Contr. Theory Appl.*, vol. 146, no. 2, pp. 171-177, March 1999.

[14] J. Lofberg, "YALMIP: A Toolbox for Modeling and Optimization in {MATLAB}", in *Proc. of the CACSD Conf.*, Taiwan, 2004. [Online]. Available: http://control.ee.ethz.ch/~joloef/yalmip.php

[15] J. F. Sturm, "Using SeDuMi 1.02, a MATLAB toolbox for optimization over symmetric cones," *Optimization Methods and Software- Special issue on Interior Point Methods*, pp. 625-653, 1999. [Online]. Available: http://sedumi.mcmaster.ca.